Stochastic models for light-scattering noise in nonlinear optical Kerr media

Robert McGraw
Rockwell International Science Center, 1049 Camino Dos Rios, Thousand Oaks, California 91360
(Received 5 August 1991)

Thermal light-scattering fluctuations are examined as a fundamental noise source inherent in nonlinear optical processes involving Kerr and artificial Kerr media. Stochastic models are introduced to simulate noise in optical phase conjugation via degenerate four-wave mixing, and in signal amplification via nondegenerate two-wave-mixing processes. Significant noise fluctuations in the amplitude and phase components of the processed signals are shown to occur even with incident signal powers in the milliwatt range. For time-dependent processes, including nondegenerate two-wave mixing, the fluctuation-dissipation theorem is shown to generalize a previously derived static susceptibility relation between light-scattering and nonlinear optical response to media exhibiting both power dissipation and nonlocal interaction.

PACS number(s): 42.50.Lc, 42.65.Hw

I. INTRODUCTION

Most treatments of optical phase conjugation and two-wave mixing do not address the role of noise; others include quantum noise in the incoming electromagnetic fields, but neglect temperature-dependent noise arising from fluctuations inherent in the nonlinear medium itself. Such fluctuations are important to consider to the extent that they reduce the fidelity of an optical signal by giving rise to scattered light.

During the past several years we have undertaken studies of light-scattering noise for cw nonlinear optical processes utilizing Kerr and artificial Kerr media [1–4] and for similar processes utilizing the photorefractive effect [5]. In the former case, a fundamental connection between light scattering fluctuations $\delta\epsilon$ in the medium and the nonlinear dielectric constant ϵ_2 was derived in the form of a static susceptibility relation [2] and was applied to a study of light-scattering noise in the phase conjugate signal obtained through degenerate four-wave mixing [3]. Time-averaged noise powers were determined and found to be of order $kT\nu$, where k is the Boltzmann constant, T is temperature, and ν is the optical frequency. At room temperature and visible wavelengths, $kT\nu$ is in the microwatt range. The static susceptibility relation between ϵ_2 and $\delta\epsilon$ was extended in a more recent paper and applied to four-wave mixing in Kerr media with nonlocal interactions near a critical point [4]. Throughout the present paper the noise arising from the fluctuations $\delta\epsilon$ is referred to equivalently as either thermal or light-scattering noise.

For many optical-signal-processing applications a more complete description of noise than is furnished by the time-averaged noise power is desired. This additional information might include, for example, the effect of light-scattering noise fluctuations on the output light intensity of a nonlinear optical device in real time. For image-processing applications, such as the use of optical phase conjugation to correct aberration, the effects of light-scattering noise on the amplitude and phase of the electromagnetic field itself must be included. In the following sections, stochastic simulations for light-scattering noise are developed; the simulations provide a direct means through which this additional information may be obtained. In Sec. II, the theory of light-scattering noise in Kerr media is extended using the fluctuation-dissipation theorem. This generalization of the static susceptibility relation is required for applications to time-dependent processes and nonlinear optical media exhibiting power dissipation. An important example of such a process, examined in Sec. IV B, is the amplification of a weak optical signal via the coherent transfer of energy from a strong pump beam during nondegenerate two-wave mixing. Section III presents the basis for stochastic noise simulation using Langevin and generalized Langevin models to relate the time decay of laser-induced gratings to the thermal fluctuations responsible for light-scattering noise. Applications to the nonlinear optical processes of phase conjugation, via degenerate four-wave mixing, and to weak signal amplification, via nondegenerate two-wave mixing, are presented in Sec. IV. Section V concludes with a summary and discussion of results.

II. GENERAL THEORY OF LIGHT-SCATTERING NOISE IN KERR MEDIA

An overview of light-scattering fluctuations and their connection to nonlinear optical response may be gained through an examination of the Maxwell equations governing beam propagation in a nonlinear medium:

$$\nabla\times\mathbf{E}(\mathbf{r},t)=-(1/c)\frac{\partial\mathbf{H}(\mathbf{r},t)}{\partial t}\ , \tag{2.1a}$$

$$\nabla\times\mathbf{H}(\mathbf{r},t)=(1/c)\frac{\partial\mathbf{D}(\mathbf{r},t)}{\partial t}\ , \tag{2.1b}$$

with

$$\mathbf{D}(\mathbf{r},t)=[\epsilon_0+\delta\epsilon(\mathbf{r},t)+\epsilon_2\bar{\mathbf{E}}^2(\mathbf{r},t)]\mathbf{E}(\mathbf{r},t)\ . \tag{2.1c}$$

In these equations, $\mathbf{E}$ ($\mathbf{H}$) is the total electric (magnetic) field vector, ϵ_0 (ϵ_2) is the linear (nonlinear) dielectric constant of the medium, $\mathbf{D}(\mathbf{r},t)$ is the displacement vector,

and the overbar implies a time average that is long compared to an optical period, but short compared to all other time scales that enter the problem. Equation (2.1c) contains both the nonlinear contribution and the fluctuation contribution to the dielectic constant. The symbols $\delta\epsilon$ and $\Delta\epsilon=\epsilon_2\bar{\mathbf{E}}^2$ are used throughout this paper to designate variations in the dielectric constant of the medium due to spontaneous fluctuations and to field-induced response, respectively. The fluctuation contribution plays a role in nonlinear optics analogous to the current or voltage fluctuations that give rise to Johnson noise in electrical systems. Both sources of noise are thermal in origin and proportional to kT. In the present case, fluctuations in the linear dielectric constant give rise to noise as they result in the formation of spontaneous gratings that are "read" by the applied laser fields to give a scattered light component that is indistinguishable from the desired output of the nonlinear optical device.

A. Light-scattering fluctuations and nonlinear optical response

At nonzero temperature T, thermal fluctuations in the linear dielectric constant of the optical Kerr medium give rise to fluctuation gratings capable of scattering incident radiation. More precisely, the fluctuations in the linear dielectric constant $\delta\epsilon(\mathbf{r},t)$ can be decomposed into grating components $\delta\epsilon(\mathbf{q},t)$:

$$\delta\epsilon(\mathbf{r},t)=\sum_{\mathbf{q}}\delta\epsilon(\mathbf{q},t)e^{-i\mathbf{q}\cdot\mathbf{r}} , \tag{2.2}$$

with

$$\delta\epsilon(\mathbf{q})=(1/V_s)\int e^{i\mathbf{q}\cdot\mathbf{r}}\delta\epsilon(\mathbf{r})d\mathbf{r} , \tag{2.3}$$

where the summation is over all grating wave vectors $\mathbf{q}$, and the integral is over the beam interaction volume V_s.

For an isotropic Kerr medium with local interactions

$$\epsilon(\mathbf{r})=\epsilon_0+\epsilon_2\bar{\mathbf{E}}^2(\mathbf{r}) \tag{2.4}$$

and Fourier transformation [cf. Eq. (2.3)] gives

$$\epsilon(\mathbf{q})=\epsilon_0\delta(\mathbf{q})+\epsilon_2\mathbf{E}^2(\mathbf{q}) . \tag{2.5}$$

A nonlocal generalization of Eq. (2.4) may be written in terms of the convolution integral [4]

$$\epsilon(\mathbf{r})=\epsilon_0+\int\epsilon_2(\mathbf{r}-\mathbf{r}')\mathbf{E}^2(\mathbf{r}')d\mathbf{r}' \tag{2.6}$$

for an isotropic medium. Fourier transformation gives

$$\epsilon(\mathbf{q})=\epsilon_0\delta(\mathbf{q})+\epsilon_2(\mathbf{q})\mathbf{E}^2(\mathbf{q}) . \tag{2.7}$$

This result is identical in form to Eq. (2.5) except for the $\mathbf{q}$ dependence in ϵ_2, which becomes important when the range of correlations in the medium approaches the wavelength of light [4].

The remainder of this section shows that the fluctuation-dissipation theorem provides a fundamental closure relation between the nonlinear coefficient ϵ_2 and the statistical distribution determining the fluctuations $\delta\epsilon$ for incorporation into Eq. (2.1c).

B. Application of the fluctuation-dissipation theorem

Preliminary to applying the fluctuation-dissipation theorem, the appropriate conjugate variables must be defined. For this purpose, it is sufficient to note that the energy change in the medium due to the nonlinear polarization is of the form

$$U(r,t)=-(1/8\pi)\Delta\epsilon(r,t)\bar{\mathbf{E}}^2(r,t) , \tag{2.8}$$

where $\Delta\epsilon$ is the change in the dielectic constant in the presence of an applied laser field. Accordingly, the field energy variable $u(r,t)=(1/8\pi)\bar{\mathbf{E}}^2$ is conjugate to $\Delta\epsilon$ and we may define the complex frequency-dependent susceptibility χ_ϵ such that

$$\Delta\epsilon(\mathbf{q},\Omega)=\chi_\epsilon(\mathbf{q},\Omega)u(\mathbf{q},\Omega) , \tag{2.9}$$

with $\chi_\epsilon=\chi'_\epsilon+i\chi''_\epsilon$. In particular, it follows from Eq. (2.9) for a Kerr medium $[\Delta\epsilon(\mathbf{q},0)=\epsilon_2(\mathbf{q})\mathbf{E}^2(\mathbf{q})]$ that $\chi_\epsilon(\mathbf{q},0)=8\pi\epsilon_2(\mathbf{q})=\chi'_\epsilon(\mathbf{q},0)$.

The power P expended by the applied fields on the medium electric polarization is proportional to the imaginary component of the susceptibility

$$P=\langle\mathbf{E}\cdot d\mathbf{P}_{\mathrm{NL}}/dt\rangle=V_s\Omega\chi''_\epsilon u^2/2 , \tag{2.10}$$

where $\mathbf{P}_{\mathrm{NL}}$ is the nonlinear polarization and the angular brackets denote averaging over the beam interaction volume V_s. The fluctuation-dissipation theorem is [6]

$$\chi''_\epsilon(\mathbf{q},\Omega)=(1/2\hbar)[1-\exp(-\hbar\Omega/kT)]S_\epsilon(\mathbf{q},\Omega) , \tag{2.11a}$$

which in the classical limit ($kT\gg\hbar\Omega$) reduces to the form

$$\chi''_\epsilon(\mathbf{q},\Omega)=(\Omega/2kT)S_\epsilon(\mathbf{q},\Omega) , \tag{2.11b}$$

where

$$S_\epsilon(\mathbf{q},\Omega)=V_s\int\langle\delta\epsilon(\mathbf{q},0)\delta\epsilon(\mathbf{q},t)\rangle e^{-i\Omega t}dt \tag{2.12}$$

is the spectral density of the fluctuations in the linear dielectric constant $\delta\epsilon$ that give rise to light scattering noise.

Each of the preceding results may readily be expressed in tensor component form for applications to anisotropic media. The scalar u, for example, is then replaced by the Maxwell stress tensor in its most general form, with $\Delta\epsilon$ and χ_ϵ represented by second- and fourth-rank tensors, respectively.

Equations (2.10)–(2.12) are the appropriate generalization of our previously derived static susceptibility relation, which was limited to degenerate beam interactions and did not include dissipation. To recover the special case, first note that the real and imaginary components of χ_ϵ satisfy the Kramers-Kronig relation [6]

$$\chi'_\epsilon(\mathbf{q},0)=(1/\pi)\int[\chi''_\epsilon(\mathbf{q},\Omega)/\Omega]d\Omega$$
$$=(kT)^{-1}V_s\langle|\delta\epsilon(\mathbf{q})|^2\rangle , \tag{2.13}$$

where the last equality follows upon substitution from Eqs. (2.11b) and (2.12) for the imaginary susceptibility component and the integral is over both positive and negative frequencies. From Eq. (2.13), and the above assign-

ment of $\chi_\epsilon(\mathbf{q},0)$ for a Kerr medium,

$$\chi'_\epsilon(\mathbf{q},0)=8\pi\epsilon_2(\mathbf{q}) , \tag{2.14}$$

the static susceptibility relation [2–4]

$$\langle|\delta\epsilon(\mathbf{q})|^2\rangle=8\pi kT\epsilon_2(\mathbf{q})/V_s \tag{2.15}$$

is immediately obtained. Equation (2.15) is the closure relation required for incorporation into Eq. (2.1c). Its present derivation is both more direct and more general than the thermodynamic fluctuation approach employed in Ref. [4], which also allows for possible $\mathbf{q}$ dependence in the Kerr coefficient due to nonlocal interaction.

For the case of photorefractive media, dielectric fluctuations arise from thermal fluctuations in the space-charge field through the electro-optic effect [5]. In this case the fluctuation variance is given by an expression

$$\langle|\delta\epsilon(\mathbf{q})|^2\rangle_{\rm PR}=(4\pi kT/\epsilon_0 V_s)[1+(q/k_D)^2]^{-1}(\varepsilon^{(2)})^2 \tag{2.16}$$

which differs from the right-hand side of Eq. (2.15) only by the nondimensional factor $(\varepsilon^{(2)})^2/2\epsilon_0\epsilon_2(0)$, where $\varepsilon^{(2)}$ is the Pockels coefficient and the $\mathbf{q}$ dependence takes the same form as that obtained previously for the nonlocal interaction described in Ref. [4], with the range of correlations set by the Debye screening length (k_D^{-1}).

III. STOCHASTIC NOISE SIMULATION MODELS

Evaluation of the spectral density of fluctuations using Eq. (2.12) requires input from the time response properties of the medium so that the autocorrelation function $\langle\delta\epsilon(\mathbf{q},0)\delta\epsilon(\mathbf{q},t)\rangle$ may be obtained. Time-response properties are also needed to obtain the frequency-dependent gain curve for the nondegenerate two-wave-mixing calculations presented in Sec. IV.

A. General model

The most general time evolution of $\delta\epsilon(\mathbf{q})$ may be modeled using a generalized Langevin form for the decay of a single hydrodynamic mode in the presence of a random force $F(t)$ representing the bath [7]:

$$\frac{\partial\delta\epsilon(\mathbf{q},t)}{\partial t}=i\Omega\delta\epsilon(\mathbf{q},t)-\int K(\tau)\delta\epsilon(\mathbf{q},t-\tau)d\tau+F(t) . \tag{3.1}$$

Here Ω is the frequency, $K(\tau)$ is the memory function, and the range of integration is from $\tau=0$ to t. Evolution of the autocorrelation function $C(t)=\langle\delta\epsilon(\mathbf{q},0)\delta\epsilon(\mathbf{q},t)\rangle$ then takes the form

$$\frac{\partial C(t)}{\partial t}=i\Omega C(t)-\int K(\tau)C(t-\tau)d\tau , \tag{3.2}$$

since $\langle\delta\epsilon(\mathbf{q},0)F(t)\rangle=0$. The random force appears implicitly in the memory function to which it is connected via the second fluctuation-dissipation theorem [7]:

$$K(t)=\langle|\delta\epsilon(\mathbf{q})|^2\rangle^{-1}\langle F(0)F(t)\rangle . \tag{3.3}$$

B. Debye relaxation model

To simplify the present treatment, a single relaxation time Debye model is used to describe the medium time response for the dielectric grating $\delta\epsilon(\mathbf{q},t)$. For this case the relaxation process is Markovian and satisfies the ordinary hydrodynamic mode decay from (Ref. [7])

$$\frac{\partial\delta\epsilon(\mathbf{q},t)}{\partial t}=-\Gamma(\mathbf{q})\delta\epsilon(\mathbf{q},t)+F(t) , \tag{3.4}$$

where $F(t)$ is the Langevin random force and $\Gamma(\mathbf{q})$ is the first-order rate constant for the grating decay. [For a diffusive process, such as the relaxation of a particle density grating in an artificial Kerr medium, $\Gamma(\mathbf{q})=Dq^2$ where D is the diffusion constant.] Equation (3.4) is a special case of the generalized Langevin form [Eq. (3.1)] achieved by setting $\Omega=0$ and $K(t)=2\Gamma(\mathbf{q})\delta(t)$, where $\delta(t)$ is the delta function. Substitution into Eq. (3.3) gives

$$\langle F(0)F(t)\rangle=2\langle|\delta\epsilon(\mathbf{q})|^2\rangle\Gamma(\mathbf{q})\delta(t) \tag{3.5}$$

as the fundamental connection between the decay constant and the mean-square fluctuations of the random force. Similar substitutions using Eq. (3.2) result in the autocorrelation function for stationary fluctuations of $\epsilon(\mathbf{q},t)$ given by

$$\langle\delta\epsilon(\mathbf{q},0)\delta\epsilon(\mathbf{q},t)\rangle=\langle|\delta\epsilon(\mathbf{q})|^2\rangle\exp[-\Gamma(\mathbf{q})t] . \tag{3.6}$$

Since, according to the Onsager regression hypothesis, the same relaxation processes govern both spontaneous fluctuation and field-induced grating decay [7], Eqs. (3.4) and (3.6) also describe the relaxation of the field-induced grating $\Delta\epsilon(\mathbf{q},t)$.

For the Debye relaxation model, substitution of Eq. (3.6) into Eq. (2.12) and carrying out the integration give

$$\begin{aligned}S_\epsilon(\mathbf{q},\Omega)&=2\tau V_s\langle|\delta\epsilon(\mathbf{q})|^2\rangle/[1+(\Omega\tau)^2]\\&=2\pi V_s G_\epsilon(\Omega) ,\end{aligned} \tag{3.7}$$

where the second equality defines the power spectrum of the time correlation for fluctuations in the dielectric grating $\delta\epsilon(\mathbf{q},t)$,

$$G_\epsilon(\Omega)=(2\pi)^{-1}\int\langle\delta\epsilon(\mathbf{q},0)\delta\epsilon(\mathbf{q},t)\rangle e^{-i\Omega t}dt , \tag{3.8a}$$

together with the inverse relation

$$C(t)=\langle\delta\epsilon(\mathbf{q},0)\delta\epsilon(\mathbf{q},t)\rangle=\int G_\epsilon(\Omega)e^{i\Omega t}d\Omega . \tag{3.8b}$$

From Eq. (3.7) we obtain

$$\int G_\epsilon(\Omega)d\Omega=\langle|\delta\epsilon(\mathbf{q})|^2\rangle . \tag{3.9}$$

Integrations are from $-\infty$ to $+\infty$ in Eqs. (3.8) and (3.9).

Equations (3.4)–(3.6) describe an Ornstein-Uhlenbech process similar in form to the relaxation of the velocity of a particle undergoing Brownian motion [8–10]. This process may be simulated [with $\delta\epsilon(\mathbf{q},t)=v(t)$] using

$$\begin{aligned}&\text{Prob}[v(t_{n+1})|v(t_n)]\\&\quad=[\sigma(h)]^{-1}(2\pi)^{-1/2}\\&\qquad\times\exp\{[v(t_{n+1})-\langle v(t_{n+1})\rangle]^2/2\sigma^2(h)\} ,\end{aligned} \tag{3.10a}$$

where

$$\sigma^2(h)=\sigma^2(\infty)[1-\exp(-2\Gamma h)] \tag{3.10b}$$

and

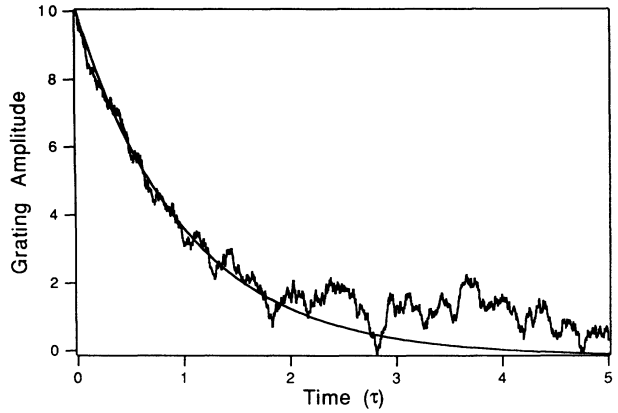

FIG. 1. Stochastic simulation of grating amplitude decay. The noise curve was obtained from the Langevin model described in the text. The smooth curve describes pure exponential decay.

$$\langle v(t_{n+1})\rangle = v(t_n)\exp(-\Gamma h)\ , \tag{3.10c}$$

with stationary variance $\sigma^2(\infty)=\langle|\delta\epsilon(\mathbf{q})|^2\rangle$. The left-hand side of Eq. (3.10a) gives the probability of finding the particular value $v(t_{n+1})$ at time step $n+1$ given that $v=v(t_n)$ at time step n. Since the process is Markovian, there is no dependence on the time origin and Eqs. (3.10) may be solved in succession for a sequence of small time steps $t=0,h,2h,3h,\ldots$ separated by $h\ll\Gamma^{-1}$.

Results from a simulation of grating decay are shown in Fig. 1. The figure shows a simulation of $\Delta\epsilon(\mathbf{q},t)$ over a time period of five reduced time units ($\tau=\Gamma^{-1}$) with the initial condition $\Delta\epsilon(\mathbf{q},0)=10.0$ standard deviations [in units of $\sigma(\infty)$] from the uniform distribution $\langle\delta\epsilon(\mathbf{q})\rangle=0$. At each time step, with h set equal to 0.0025 reduced time units for the calculation, the probability distribution defined by Eq. (3.10a) was sampled using a standard computer subroutine incorporating the Box-Muller transformation for the generation of normal deviates from random numbers sampled uniformly on the interval (0,1) [11]. Superimposed on the stochastic simulation is the function $\langle\Delta\epsilon(\mathbf{q},t)\rangle=\langle\Delta\epsilon(\mathbf{q},0)\rangle\exp(-\Gamma t)$ shown as the smooth curve in the figure. This function is seen to provide a good description of the average grating decay. At long times, memory of the initial grating is lost and the typical stationary grating fluctuations due to thermal noise may be seen.

IV. APPLICATIONS TO NONLINEAR OPTICAL PROCESSES

The simulation of noise in nonlinear optical processes requires that the fluctuations $\delta\epsilon(\mathbf{q},t)$ be incorporated into the Maxwell equations governing beam propagation in the nonlinear medium. The general wave equation for the nonlinear medium, with the noise fluctuations $\delta\epsilon$ included, follows from Eqs. (1):

$$\nabla^2\mathbf{E}(\mathbf{r},t)=-(\omega^2/c^2)(\epsilon_0+\epsilon_2\overline{\mathbf{E}}^2+\delta\epsilon)\mathbf{E}(\mathbf{r},t)\ , \tag{4.1}$$

where $\mathbf{E}(\mathbf{r},t)$ is the total electric field. The solutions to Eq. (4.1) will now be obtained for two-wave- and four-wave-mixing processes. For calculations in the time domain a sequence of values of $\delta\epsilon$ is generated numerically, as described above in connection with Fig. 1, and a solution to Eq. (4.1) is obtained for each member of the sequence. The resulting fluctuations in the electromagnetic field describe the effects of light-scattering noise in the time domain. An important point is that the field fluctuations will track the dielectric fluctuations $\delta\epsilon$ adiabatically, since the latter vary on a time scale ($\tau=\Gamma^{-1}$) set by the medium response, which is slow compared to the transit time of light through the medium. Accordingly, only the instantaneous value of $\delta\epsilon$ is required to obtain a solution valid over a time interval that is short compared to the response time of the medium. This adiabatic approximation provides the physical basis for the stochastic simulations presented below.

A. Optical phase conjugation via degenerate four-wave mixing

Figure 2 shows a standard four-wave-mixing geometry used to obtain optical phase conjugation of a probe signal $\mathbf{E}_p$. For this case, the total electromagnetic field entering into Eq. (4.1) takes the form

$$\mathbf{E}(\mathbf{r},t)=\tfrac{1}{2}[(\mathbf{e}_pE_pe^{i\mathbf{Q}\cdot\mathbf{r}}+\mathbf{e}_cE_ce^{-i\mathbf{Q}\cdot\mathbf{r}} +\mathbf{e}_1E_0e^{i\mathbf{K}\cdot\mathbf{r}}+\mathbf{e}_2E_0e^{-i\mathbf{K}\cdot\mathbf{r}})e^{-i\omega t}+\text{c.c.}]\ , \tag{4.2}$$

where $\mathbf{e}_j$, E_j, $\mathbf{K}_j$, and ω are, respectively, the unit polarization vector, electric-field amplitude, wave vector, and frequency for wave j. Here the two counterpropagating pump beams are taken to have equal amplitudes, $E_1=E_2=E_0$, and E_p and E_c are the slowly varying envelopes of the probe and conjugate waves. The figure also shows transmitted probe at $z=L$ and a set of signal $[\Delta\epsilon(\mathbf{q})]$ and noise $[\delta\epsilon(\mathbf{q})]$ gratings, represented respectively by the solid and dashed sinusoidal curves, contributing to the conjugate wave. Here $\mathbf{q}=\mathbf{K}-\mathbf{Q}$ for the field-induced grating formed in the interaction volume of

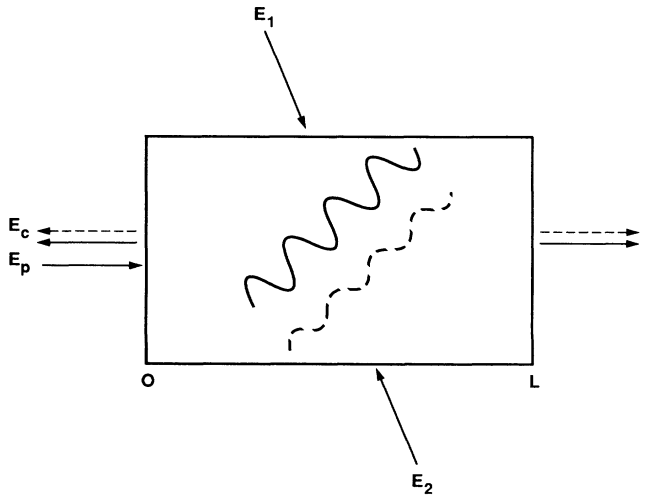

FIG. 2. Four-wave-mixing geometry.

the incident probe and one of the pump beams ($\mathbf{E}_1$). For parallel beam polarizations there will also be an orthogonal grating, of wave vector $\mathbf{q}=\mathbf{K}-\mathbf{Q}$, not shown in the figure. Only those thermal gratings (such as the one depicted in the figure) that give a scattered-light component in the direction and frequency range of the conjugate wave (so as to be indistinguishable from the conjugate wave) constitute a true source of noise [3]. Solid (dashed) arrows represent the signal (noise) contribution to the conjugate and to the transmitted probe.

Solutions to Eqs. (4.1) and (4.2) that include the effects of light scattering both on beam attenuation (nonsaturable background loss) and on noise are given in Ref. [4] for a fluid medium near its critical point. To simplify matters, the solutions are given here first neglecting beam attenuation as was done in Ref. [3] for calculations of the time-averaged noise power. In addition, we shall assume that the medium is isotropic and that all of the incident radiation is linearly polarized in the same direction. The role of nonsaturable background loss is discussed further at the end of this section.

Substitution of Eq. (4.2) into Eq. (4.1) and use of the slowly varying envelope and phase approximation give [3]

$$\frac{dE_p^*(z)}{dz}=-i\kappa_0(E_p^*+E_c)-i\mathcal{L}\ , \tag{4.3a}$$

$$\frac{dE_c(z)}{dz}=-i\kappa_0(E_p^*+E_c)-i\mathcal{L}\ , \tag{4.3b}$$

where the positive z coordinate is taken to lie in the direction of the probe wave vector $\mathbf{Q}$. In Eqs. (4.3), $\kappa_0=\epsilon_2 Q E_0^2/2\epsilon_0$ is the four-wave-mixing coefficient and

$$\mathcal{L}=QE_0[\delta\epsilon(-\mathbf{K}-\mathbf{Q})+\delta\epsilon(\mathbf{K}-\mathbf{Q})]/2\epsilon_0 \tag{4.4}$$

is the noise operator [3].

Equations (4.3) were previously solved for the conjugate and transmitted probe intensity after a time averaging of the fluctuations appearing in Eq. (4.4) was performed [3]. However, the solutions to Eqs. (4.3) for the probe and conjugate field at fixed $\mathcal{L}$ are also readily obtained. These are

$$E_p^*(z)=e^{-i\kappa_0 z}\cos(\kappa_0 z)E_p^*(0) -ie^{-i\kappa_0 z}\sin(\kappa_0 z)[E_c(0)+(\mathcal{L}/\kappa_0)]\ , \tag{4.5a}$$

$$E_c(z)=e^{-i\kappa_0 z}\cos(\kappa_0 z)E_c(0) -ie^{-i\kappa_0 z}\sin(\kappa_0 z)[E_p^*(0)+(\mathcal{L}/\kappa_0)]\ , \tag{4.5b}$$

as may be readily verified by differentiation. The boundary conditions are determined by the values of the incident fields, which are $E_p^*(0)$ at $z=0$ and $E_c(L)$ at $z=L$, where L is the beam interaction length. From Eq. (4.5b) we obtain

$$E_c(0)=E_c(L)e^{i\kappa_0 L}\sec(\kappa_0 L) +i\tan(\kappa_0 L)[E_p^*(0)+(\mathcal{L}/\kappa_0)]\ . \tag{4.6}$$

Substitution of this last result into Eqs. (4.5) yields expressions for $E_p^*(z)$ and $E_c(z)$ in terms of the incident fields In the present analysis we consider the solution for the conjugate field $E_c(0)$ subject to the usual boundary condition $E_c(L)=0$ for which case

$$E_c(0)=[E_p^*(0)+\mathcal{L}/\kappa_0]i\tan(\kappa_0 L)\ . \tag{4.7}$$

Equation (4.7) gives a recovery of the usual noise-free result for $\mathcal{L}=0$ [12].

The analytic solutions given above were obtained assuming fixed values for the amplitude and phase of the complex noise operator $\mathcal{L}$. However, Eqs. (2.15) and (4.4) show that $\mathcal{L}$ undergoes Gaussian fluctuations in time with

$$\langle|\mathcal{L}|^2\rangle=(Q^2E_0^2/4\epsilon_0^2)\langle|\delta\epsilon(-\mathbf{K}-\mathbf{Q})+\delta\epsilon(\mathbf{K}-\mathbf{Q})|^2\rangle =2(Q^2E_0^2/4\epsilon_0^2)8\pi kT\epsilon_2(\mathbf{q})/V_s \tag{4.8}$$

and random phase. The factor of 2 in the last equality arises because we are computing the variance of a sum of two independent variables having the same density distribution. Inspection of Eqs. (4.7) and (4.8) reveals that the noise properties of the conjugate wave are largely independent of specific physical properties of the nonlinear medium, but are dependent, instead, only on the general conditions of optical frequency, probe beam total power, temperature, and phase-conjugate reflectivity (R) through the relation $R=\tan^2(\kappa_0 L)$.

To make further progress, we observe that the fluctuations in $\mathcal{L}$ (due to fluctuations in $\delta\epsilon$) vary on the time scale set by the medium response, which is slow compared to the transit time of light through the medium. As indicated at the beginning of the section, this adiabatic approximation provides an especially convenient basis for utilizing the stochastic models presented in Sec. III to simulate the effects of light-scattering noise. As the principal method employed in the calculations that follow, the generated sequence $\delta\epsilon(t)$ is sampled at time intervals that are long compared to the medium response time (τ). Each sampled value is then statistically independent from the preceding one. Specifically, this approach consists of obtaining the solution to Eq. (4.1) separately for each fixed-$\delta\epsilon$ or, equivalently, fixed-$\mathcal{L}$ member of a statistical ensemble. The ensemble itself is defined to consist of the collection of solutions obtained for a representatively large sample of statistically independent values of $\delta\epsilon$ for each noise grating. (In the present case both the $\mathbf{K}+\mathbf{Q}$ and the $\mathbf{K}-\mathbf{Q}$ gratings contribute separately to the signal and to the noise components of the conjugate wave.) Each set of $\delta\epsilon$ values is generated through computer sampling to have Gaussian statistics characterized by Eqs. (2.15) and (3.7), and to satisfy the condition of random phase. Corresponding $\mathcal{L}$ values have Gaussian statistics characterized by Eq. (4.8). The sampling procedure employs the same random number generation algorithm as previously used for the simulation of grating decay in Sec. III B [11]. The interaction volume V_s appearing in

Eq. (4.8) is obtained as the product of the probe-beam cross-section area (A) and the interaction length (L).

Results from stochastic noise simulation for the conjugate field are shown in Figs. 3 and 4 for a wavelength of 1.06 μm and phase conjugate reflectivity near unity. As noted above, these results are independent of changes in the pump power, provided that κ_0 and L are chosen such that the phase-conjugate reflectivity is the same. Figure 3 shows the distribution of amplitude and phase fluctuations in the conjugate field due to light-scattering noise. Without loss of generality, the incident probe field is taken to be real and is represented by the single point appearing on the real axis in the figure. A representative set of 500 values of $\mathcal{L}$ were generated in the manner described above, and the real and imaginary components for the corresponding E-field solutions given by Eq. (4.7) were plotted in the figure. The resulting cluster of points is centered on the noise-free (zero-temperature) solution obtained by setting $\mathcal{L}=0$. The latter lies on the imaginary axis due to a phase shift of $\pi/2$ incurred in forming the conjugate wave. The variance of the scatter is directly proportional to temperature (here set at 300 K) and inversely proportional to total probe power (here set at 1 mW), but is not dependent separately on the probe-beam cross-sectional area (A) or probe intensity. A useful figure of merit is the dimensionless ratio $F=P_p/kT\nu$, where P_p is the total probe power. For constant values of F and phase-conjugate reflectivity, probability scatter plots of the type shown in Figs. 3 and 4 (below) appear identical except for scaling.

The scatter shown in Fig. 3 implies a corresponding level of noise in the conjugate wave form itself. Restoring the $\exp(-i\omega t)$ temporal dependence from Eq. (4.2)

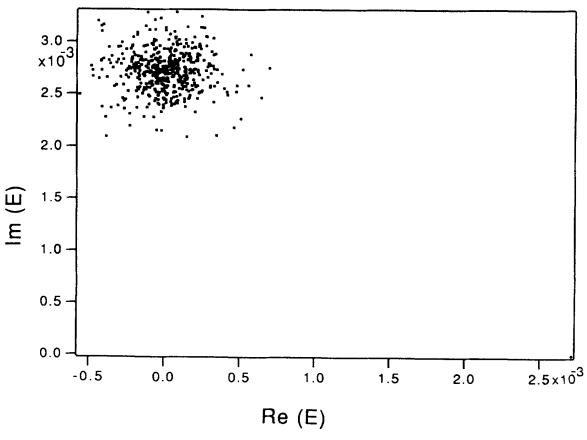

FIG. 3. Fluctuations in the real and imaginary components of the conjugate field due to light-scattering noise. Simulation is for a wavelength of 1.06 μm, incident probe power of 1 mW, temperature of 300 K, and phase-conjugate reflectivity near unity. The incident noise-free probe wave is taken to be real and is represented by the single dot appearing in the lower right-hand corner of the figure. Note that the conjugate wave, represented by the cluster of points in the figure, is shifted in phase from the probe by 90°. Field amplitudes are expressed in cgs units.

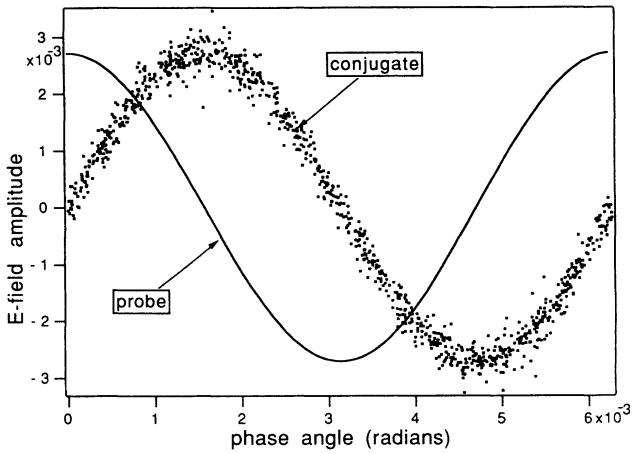

FIG. 4. Wave forms for the noise-free probe and conjugate waves under the same conditions as for Fig. 3.

gives

$$E_c(0)=E_R\cos(\omega t)+E_I\sin(\omega t)\ , \tag{4.9}$$

where E_R and E_I are the real and imaginary components, respectively, whose distribution is shown in Fig 3. If we neglect quantum noise fluctuations in the incident beams, the wave form for the monochromatic probe beam at $z=0$ has pure cosine form with fixed amplitude and is plotted as a function of the phase angle (ωt) in Fig. 4. For the conjugate wave, on the other hand, each set of coordinates (E_R,E_I) from Fig. 3 produces a separate wave form in Fig. 4. Rather than drawing many such complete wave forms to represent the noisy conjugate wave, we instead randomly select a single point on each wave form, through a random selection of phase over the interval $(0,2\pi)$, and plot this point alone. A 1000 point sampling (one point from each wave form) generates a probabilistic representation of the conjugate wave amplitude and phase as shown in Fig. 4. Note that while exhibiting considerable uncertainty in its amplitude and phase, the conjugate wave-form distribution remains stationary in time. Thus, instead of a pure sinusoidal form, the E-field vector for the noisy conjugate wave lies within a stationary probability distribution centered on the zero-temperature conjugate wave form. Applying the superposition principle, we see that a complicated probe signal, represented as a sum of sinusoidal waves with different amplitudes and phases, will give rise to a conjugate signal consisting of a sum of correspondingly broadened wave forms and consequent information loss. In addition, the repassage of such broadened wave forms through an aberrator would clearly result in less-than-perfect correction of image distortion. These results highlight the importance of light-scattering noise in four-wave mixing.

Figure 5 shows the effect of including light-scattering attenuation in the equations for four-wave mixing. The resulting gain curves for phase-conjugate reflectivity are centered on the usual noise-free results. The figure indicates that the largest effects of beam attenuation are a reduction of the overall gain in a manner that is largely

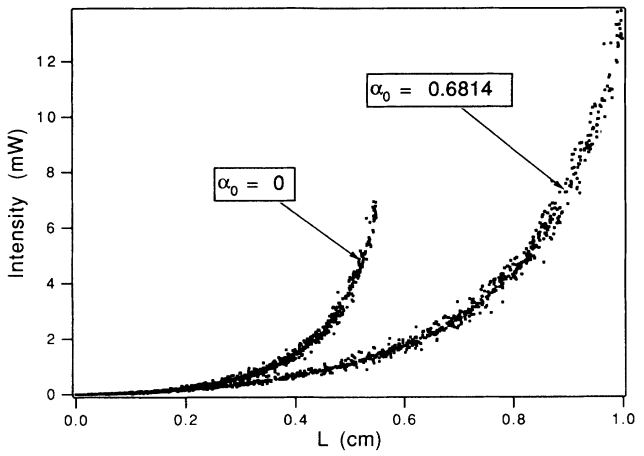

FIG. 5. Noise fluctuations in the conjugate power as a function of the beam interaction length. Conditions are the same as for Fig. 3 with $\kappa_0=2.18$ cm^{-1}. The two simulations compare the effects of including, vs not including, beam attenuation due to scattering for an isotropic Kerr medium.

independent of the noise. Thus light scattering has two effects: (1) It limits gain due to reduction in signal and pump beam intensities through attenuation. This has been shown to result in an optimum beam interaction length for maximum phase-conjugate reflectivity. (2) Light scattering is the manifestation of thermal noise inherent in the medium. Since these effects are essentially independent of each other, light scattering may be treated as a contributory source of beam attenuation (beam loss due to absorption may also occur), without including light scattering as noise. Similarly, e.g., at longer wavelengths, the effects of light-scattering noise may be included and beam attenuation may be neglected if the scattering losses are small. This separation is possible because the scattering attenuation and noise properties each have different dependences on the wavelength of light.

B. Nondegenerate two-wave mixing

For the treatment of light-scattering noise in degenerate four-wave mixing, it was sufficient to use the static susceptibility relation given by Eq. (2.15) to evaluate the thermal fluctuations. The analogous treatment for nondegenerate two-wave mixing requires a more detailed model in order to include the time-dependent response properties of the medium and of the fluctuations that give rise to noise. Thus, to obtain the noise in two-wave mixing, the general fluctuation-dissipation relation embedded in Eqs. (2.10)–(2.12) is required. Results are presented in this section for the case of a Debye relaxation Kerr medium with time-dependent dielectric response characteristics described in Sec. III B. As a more complete discussion of light-scattering noise incurred during two-wave mixing gain is planned for future publication, the treatment given below will be limited to showing specifically how the theoretical framework developed in Secs. II and III is applied to the two-wave-mixing noise case.

A schematic illustration of the two-wave-mixing geometry for amplification of a weak signal is shown in Fig. 6. Two laser beams of frequencies ω_1 and $\omega_2=\omega_1-\Omega$ propagate through the nonlinear medium and create a moving density grating response that preferentially deflects energy from the high-frequency to the low-frequency beam. The solid lines depict the crests of the field-induced grating of wave vector $\mathbf{q}=\mathbf{K}_1-\mathbf{K}_2$. Dashed lines represent a spontaneous moving grating arising from thermal fluctuations in the medium. Some of these thermal gratings will be in a proper configuration to deflect energy from the high-frequency to the low-frequency wave, in a manner that is indistinguishable from the signal, to give a noise component represented by the dashed arrow in the figure. For two incident plane waves the total field is of the form

$$\mathbf{E}(\mathbf{r},t)=\mathbf{e}_1E_1(\mathbf{r})\cos[\mathbf{K}_1\cdot\mathbf{r}-\omega_1t+\theta_1(\mathbf{r})] + \mathbf{e}_2E_2(\mathbf{r})\cos[\mathbf{K}_2\cdot\mathbf{r}-\omega_2t+\theta_2(\mathbf{r})] , \quad (4.10)$$

where $\mathbf{e}_j$, $E_j(\mathbf{r})$, and $\theta_j(\mathbf{r})$ are the unit polarization vector, slowly varying amplitude, and slowly varying phase of wave j.

The signal and noise gratings depicted schematically in Fig. 6 are quantitatively described as follows: For the signal grating [13]

$$\Delta\epsilon(\mathbf{r},t)=a_1\cos(\mathbf{q}\cdot\mathbf{r}-\Omega t)+b_1\sin(\mathbf{q}\cdot\mathbf{r}-\Omega t) , \quad (4.11)$$

where

$$a_1=(\mathbf{e}_1\cdot\mathbf{e}_2)\epsilon_2E_1E_2/[1+(\Omega\tau)^2] \quad (4.12)$$

and

$$b_1=-(\mathbf{e}_1\cdot\mathbf{e}_2)\epsilon_2E_1E_2\Omega\tau/[1+(\Omega\tau)^2] \quad (4.13)$$

are the in-phase and $\pi/2$ out-of-phase grating coefficients, respectively, for a Debye relaxation medium.

For the noise gratings, the coefficients a_Ω and b_Ω are statistically distributed and may be obtained through an

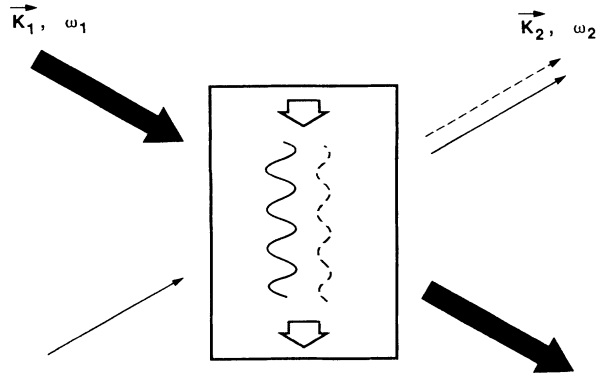

FIG. 6. Two-wave-mixing geometry.

analysis of the dielectric fluctuations $\delta\epsilon(\mathbf{r},t)$. For this purpose, a grating fluctuation, with time correlation function given by Eq. (3.6), may be represented in the form

$$\delta\epsilon(\mathbf{r},t)=A(t)\cos(\mathbf{q}\cdot\mathbf{r}) , \tag{4.14}$$

where $A(t)$ is a stationary random variable in time whose time-correlation function

$$\langle A(0)A(t)\rangle=\langle |A|^2\rangle \exp[-\Gamma(\mathbf{q})t] \tag{4.15}$$

with

$$\langle |A|^2\rangle=2\langle |\delta\epsilon(q)|^2\rangle \tag{4.16}$$

follows from a comparison of Eqs. (3.6) and (4.14).

The properties of random variables of the type described by Eqs. (4.15) and (4.16) are well known. In particular, $A(t)$ may be decomposed into temporal Fourier components with amplitudes whose statistical properties are given in Ref. [14]:

$$A(t)=\int d\Omega[\alpha_\Omega\cos(\Omega t)+\beta_\Omega\sin(\Omega t)] . \tag{4.17}$$

Integration is over positive values of the frequency Ω and the coefficients α and β are Gaussian random variables with [10]

$$\langle\alpha\rangle=\langle\beta\rangle=0 \tag{4.18}$$

and

$$\langle\alpha_\Omega^2\rangle=\langle\beta_\Omega^2\rangle=(2\tau/\pi)\langle |A|^2\rangle/[1+(\Omega\tau)^2] , \tag{4.19}$$

where $\tau=\Gamma^{-1}$ is the response time of the Debye relaxation medium.

To accomplish the decomposition of Eq. (4.14) into moving gratings, simply substitute for $A(t)$ from Eq. (4.17) and use standard trigonometric identities to obtain

$$\delta\epsilon(\mathbf{r},t)=\int d\Omega[a_\Omega\cos(\mathbf{q}\cdot\mathbf{r}-\Omega t)+b_\Omega\sin(\mathbf{q}\cdot\mathbf{r}-\Omega t)] , \tag{4.20}$$

where $a_\Omega=a_{-\Omega}=\alpha_\Omega/2$, $b_\Omega=-b_{-\Omega}=\beta_\Omega/2$, and the integration is now over both positive and negative frequencies. From these relations the mean and variances for the fluctuating grating coefficients a_Ω and b_Ω are immediately obtained:

$$\langle a_\Omega\rangle=\langle b_\Omega\rangle=0 , \tag{4.21}$$

$$\langle a_\Omega^2\rangle=\langle b_\Omega^2\rangle=(\tau/\pi)\langle |\delta\epsilon(\mathbf{q})|^2\rangle/[1+(\Omega\tau)^2] . \tag{4.22}$$

Comparison with Eqs. (3.7) and (3.9) shows that the right-hand side of Eq. (4.22) gives the noise power on a per unit angular frequency basis. To obtain the noise power per hertz, simply multiply this expression by 2π. It is useful to express the fluctuation variance in a manner that is independent of medium response time τ. To do this, we express frequency shifts nondimensionally in units of $\Omega\tau$ and, in place of Eqs. (4.21) and (4.22), introduce scaled noise grating coefficients $\bar{a}_\Omega$ and $\bar{b}_\Omega$ with the properties

$$\langle\bar{a}_\Omega\rangle=\langle\bar{b}_\Omega\rangle=0 \tag{4.23}$$

and

$$\langle\bar{a}_\Omega^2\rangle=\langle\bar{b}_\Omega^2\rangle=\langle |\delta\epsilon(\mathbf{q})|^2\rangle/[1+(\Omega\tau)^2]$$
$$=(8\pi kT\epsilon_2/V_s)/[1+(\Omega\tau)^2] , \tag{4.24}$$

where the last equality follows from Eq. (2.15). Comparison with Eqs. (3.7) and (3.9) shows that the right-hand side of Eq. (4.24) gives the fluctuation variance for a signal collection bandwidth $\Delta\Omega=\pi/\tau$. Upon setting the beam interaction volume V_s equal to the product of the cross section area (A) and interaction length (L), each of the quantities appearing in this expression is determined.

Having obtained expressions for the field-induced and the fluctuation grating components, we turn now to the solution of the Maxwell equations for the two-wave-mixing case. For this purpose, Eqs. (4.11) and (4.20) may be combined to obtain an expression for the total variation in dielectric constant from both signal and noise. When the result is substituted into the wave equation, the various terms in the displacement vector give rise to scattering of electromagnetic energy into different modes, characterized by specific wave vectors and frequencies. The most significant contribution results from those terms that have minimum phase mismatch. Denoting these by $\mathbf{D}(\mathbf{r},t)$, we find

$$\mathbf{D}(\mathbf{r},t)=\epsilon_0\mathbf{E}(\mathbf{r},t)+\tfrac{1}{2}(a_1+a_\Omega)E_1(\mathbf{r})\cos(\mathbf{K}_2\cdot\mathbf{r}-\omega_2 t+\theta_2)\mathbf{e}_1+\tfrac{1}{2}(a_1+a_\Omega)E_2(\mathbf{r})\cos(\mathbf{K}_1\cdot\mathbf{r}-\omega_1 t+\theta_1)\mathbf{e}_2$$
$$-\tfrac{1}{2}(b_1+b_\Omega)E_1(\mathbf{r})\sin(\mathbf{K}_2\cdot\mathbf{r}-\omega_2 t+\theta_2)\mathbf{e}_1+\tfrac{1}{2}(b_1+b_\Omega)E_2(\mathbf{r})\sin(\mathbf{K}_1\cdot\mathbf{r}-\omega_1 t+\theta_1)\mathbf{e}_2 , \tag{4.25}$$

where a_1 and b_1 are fixed and field dependent, while a_Ω and b_Ω are field-independent fluctuating quantities. Equation (4.25) describes an instantaneous polarization, or snapshot of the medium, that includes contributions from both signal and phase-matched noise gratings. According to the adiabatic approximation, described above, the polarizability will remain constant over time periods that are short when compared with the medium response time $\tau=\Gamma^{-1}$, yet long when compared with the transit time of light through the medium.

Inserting Eq. (4.25) into the wave equation [Eq. (4.1)], making the slowly varying amplitude and phase approximation, and equating the in-phase and out-of-phase terms, one finds

$$(\mathbf{K}_1\cdot\nabla)E_1=(K^2/4\epsilon_0)(b_1+b_\Omega)(\mathbf{e}_1\cdot\mathbf{e}_2)E_2-(\alpha_0/2)E_1 , \tag{4.26a}$$

$$(\mathbf{K}_1\cdot\nabla)\theta_1=(K^2/4\epsilon_0)(a_1+a_\Omega)(\mathbf{e}_1\cdot\mathbf{e}_2)E_2/E_1 \tag{4.26b}$$

for the pump wave and

$$(\mathbf{K}_2\cdot\nabla)E_2=-(K^2/4\epsilon_0)(b_1+b_\Omega)(\mathbf{e}_1\cdot\mathbf{e}_2)E_1-(\alpha_0/2)E_2\ , \tag{4.26c}$$

$$(\mathbf{K}_2\cdot\nabla)\theta_2=(K^2/4\epsilon_0)(a_1+a_\Omega)(\mathbf{e}_1\cdot\mathbf{e}_2)E_1/E_2 \tag{4.26d}$$

for the signal. These equations are identical to those obtained previously [13,15] except for the presence of the new noise terms, which result in fluctuations in both amplitude and phase. When the pump is much stronger than the signal ($E_1 \gg E_2$), these fluctuations are much more important for the signal than for the pump beam. The last terms in Eqs. (4.26a) and (4.26c) include the effect of nonsaturable background loss, where α_0 is the attenuation coefficient for loss of light intensity. For a nonabsorbing medium in which losses are due to scattering alone,

$$\alpha_0=(\omega^4/6\pi c^4)V_s\langle|\delta\epsilon(\mathbf{q})|^2\rangle=\tfrac{4}{3}(2\pi\nu/c)^4kT\epsilon_2 \tag{4.27}$$

for an isotropic medium [16].

Finally, an expression for the power dissipated in the medium during two-wave mixing may be obtained [15]. For a uniformly moving grating, the stored energy in the medium is constant and the dissipated power per unit volume is

$$\mathcal{P}=\left\langle\mathbf{E}\cdot\frac{d\mathbf{P}}{dt}\right\rangle=-(1/16\pi)b_1(\mathbf{e}_1\cdot\mathbf{e}_2)E_1E_2\Omega\ , \tag{4.28}$$

where Eqs. (4.10), (4.25), and (4.26) have been used. As expected, the fluctuating noise gratings make no contribution to power dissipation.

Since α_Ω and b_Ω are fluctuating amplitudes, a computer-generated ensemble of solutions [one solution for each sampled (a_Ω,b_Ω) pair] is required to obtain a good statistical representation of the amplitude and phase fluctuations present in the propagating fields during two-wave mixing. The calculations presented below were carried out using Runge-Kutta integration of Eqs. (4.26) for each sampled Gaussian coefficient pair. Sampling was performed as previously described with all results expressed in terms of the scaled noise variables $(\bar{a}_\Omega,\bar{b}_\Omega)$ defined by Eqs. (4.23) and (4.24).

The effect of light-scattering noise during the amplification of a weak signal field via two-wave mixing is shown in Fig. 7. The figure shows the real and imaginary components of the transmitted signal for several different interaction lengths (L) ranging from 0 to 1.0 cm. The simulation does not include any noise present in the incoming signal (at $z=0$), so all of the scatter seen in the figure is due to noise generated in the medium itself. Thus there is no noise for the trivial case ($L=0$) of a vanishing beam interaction length. The specific conditions chosen for the calculation are indicated in the figure caption, although it will be shown elsewhere that the results are largely independent of the specific properties of the medium, depending instead on such general properties as temperature and power present in the incoming signal beam. (Similar properties have already been found for the four-wave-mixing case as noted above.) Note that the Kerr coefficient $\epsilon_2=1.0\times10^{-6}$ cm^3/erg ($n_2=7.3\times10^{-13}$ m^2/W) is typical of that for an artificial Kerr medium.

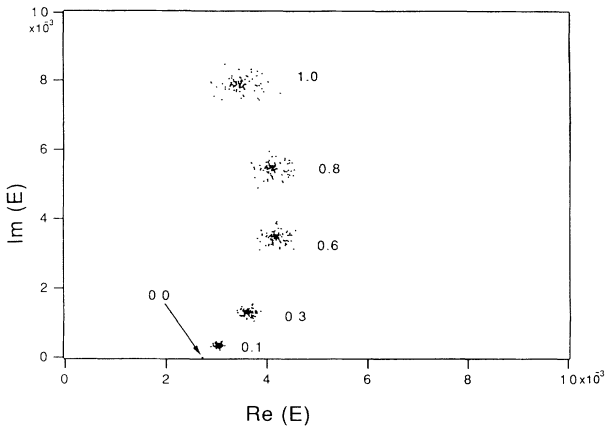

FIG. 7. Noise fluctuations in the probe amplified by two-wave mixing for several different beam interaction lengths. Specific conditions chosen for the calculation are incident signal power $P_2(0)=1$ mW, $\epsilon_2=1.0\times10^{-6}$ cm^3/erg, $\lambda=0.5$ μm, $I_{\text{pump}}=10$ kW/cm^2, and $T=300$ K. Values of the beam interaction length (in cm) are indicated in the figure. Field amplitudes are expressed in cgs units.

The amount of scatter is dependent on the signal observation bandwidth. Since the scaled noise variables defined by Eqs. (4.23) and (4.24) were used, the figure depicts noise fluctuations for an angular-frequency signal collection bandwidth equal to π/τ. For each sampled pair of noise grating coefficients $(\bar{a}_\Omega,\bar{b}_\Omega)$ incorporated into Eqs. (4.26), a unique and separate solution to these equations is obtained. For each of the five interaction lengths included in the figure, 100 sampled values of the coefficient pairs $\bar{a}_\Omega$ and $\bar{b}_\Omega$ were used. Each of the resulting clusters of points is centered on the usual solution for the noise-free ($T=0$) case. To preserve the generality of the results obtained, the effect of beam attenuation was not included in the calculation; i.e., α_0 was set equal to zero in Eqs. (4.26). Thus the results shown in Fig. 7 scale for a wide range of different conditions and are largely independent of the specific physical parameters of the nonlinear medium.

Experiments designed to verify these theoretical predictions are underway using an artificial Kerr suspension of shaped polytetrafluoroethylene (PTFE) microparticles as the active nonlinear medium [17].

V. SUMMARY

A general treatment of light-scattering noise in Kerr media has been developed based on the fluctuation-dissipation theorem and has been applied to the nonlinear optical processes of two-wave and four-wave mixing. The most general finding is that light-scattering noise is the manifestation of thermal fluctuations inherent in the nonlinear medium, while the fluctuation-dissipation theorem provides the quantitative relation between these fluctuations and the size and frequency dependence of the Kerr coefficient ϵ_2. General numerical methods for the computer simulation of beam propagation in nonlinear media have been presented using a stochastic model to incorpo-

rate the effects of noise. In the absence of thermal noise ($T=0$), the usual solutions to the Maxwell equations for two-wave- and four-wave-mixing processes are recovered.

In the case of four-wave mixing, conjugate-wave fidelity has been shown to be reduced by amplitude and phase fluctuations due to light-scattering noise. These fluctuations, seen clearly at 1-mW signal power levels in Figs. 3–5, are dependent on the total power in the probe beam and on other general characteristics of the phase-conjugate mirror, such as its temperature and thickness—corresponding to the beam interaction length L. A future publication will show that the stochastic noise models developed here can be readily used to obtain quantitative light-scattering noise limits to squeezed light generation via four-wave mixing in Kerr media.

Simulations of light-scattering noise in nondegenerate two-wave mixing also show significant amplitude and phase fluctuations at 1-mW signal power levels (Fig. 7). As was found for four-wave mixing, the noise levels obtained from two-wave mixing are largely independent of the specific material properties of the nonlinear medium. Simulation of light-scattering noise in two-wave mixing requires an additional model for the time-dependent response properties of the nonlinear medium. The resulting level of noise is dependent on both the frequency difference between the two beams and on the bandwidth of observation. For the calculations presented in this paper, a single relaxation time Debye model for the medium response was employed.

In addition to these specific applications to optical phase conjugation and two-wave mixing, a more universal role for classical light scattering in nonlinear optical processes is implied by the results of the present study. Specifically, light-scattering fluctuations have been introduced directly in the Maxwell equations governing beam propagation, and have been shown to have a much more significant role than just as a source of beam attenuation. These fluctuations have now been related quantitatively to nonlinear optical response through the fluctuation-dissipation theorem and, as such, are the manifestation of thermal noise in all nonlinear optical processes based on Kerr-type nonlinear media.

ACKNOWLEDGMENT

This research was supported by the U.S. Air Force under Contract No. F29601-89-C-0085.

[1] R. McGraw and D. Rogovin, SPIE **739**, 100 (1987).

[2] R. McGraw and D. Rogovin, in *Advances in Laser Science–III,* Proceedings of the Third International Conference, Atlantic City, New Jersey, 1987, edited by Andrew C. Tam, James L. Gole, and William C. Stwalley, AIP Conf. Proc. No. 172 (AIP, New York, 1988), p. 253.

[3] R. McGraw, D. Rogovin, and A. Gavrielides, Appl. Phys. Lett. **54**, 199 (1989).

[4] R. McGraw, Phys. Rev. A **42**, 2235 (1990).

[5] R. McGraw, in OSA 1990 Technical Digest Series, Vol. II, Optical Society of America 1988 Annual Meeting (Optical Society of America, Santa Clara, CA, 1988), paper THU3.

[6] D. Forster, *Hydrodynamic Fluctuations, Broken Symmetry, and Correlation Functions* (Benjamin, Reading, MA, 1975), Chap. 2.

[7] B. J. Berne and R. Pecora, *Dynamic Light Scattering* (Wiley, New York, 1976), Chap. 11.

[8] R. Serra, M. Andretta, M. Compiani, and G. Zanarini, *Introduction to the Physics of Complex Systems* (Pergamon, New York, 1986).

[9] G. E. Uhlenbeck and L. S. Ornstein, Phys. Rev. **36**, 823 (1930).

[10] J. D. Eversole, A. D. Kersey, A. Dandridge, and R. G. Priest, J. Opt. Soc. A **4**, 1220, 1987.

[11] W. H. Press, B. P. Flannery, S. A. Teukolsky, and W. T. Vetterling, *Numerical Recipes* (Cambridge University Press, New York, 1986), p. 203.

[12] A. Yariv and D. Pepper, Opt. Lett. **1**, 16 (1978).

[13] Y. Silberberg and I. Bar-Joseph, J. Opt. Soc. Am. B **1**, 662 (1984).

[14] N. Davidson, *Statistical Mechanics* (McGraw-Hill, New York, 1962), Chap. 14.

[15] R. McGraw and D. Rogovin, Phys. Rev. A **35**, 1181 (1987).

[16] L. D. Landau and E. M. Lifshitz, *Electrodynamics of Continuous Media* (Pergamon, New York, 1960), p. 389.

[17] R. Pizzoferrato, R. McGraw, and D. Rogovin (unpublished).